Research Article GU J Sci 38(4): 1703-1719 (2025) DOI: 10.35378/gujs.1521093

Gazi University

Journal of Science

http://dergipark.org.tr/gujs

Organic and Inorganic Sol-Gel Routes for Preparing Mesoporous γ-Alumina Powder

Orhan OZCAN[1,2*], Ayse Nilgun AKIN[1,2]

[1]*Kocaeli University, Department of Chemical Engineering, 41001, Kocaeli, Türkiye*
[2]*Kocaeli University, Alternative Fuels R&D Center, 41001, Kocaeli, Türkiye*

Highlights

- γ-Al_2O_3 powders are synthesized by using initial precursors of $AlCl_3$ and AIP.
- BET surface areas are reported as 209-299 m^2/g (inorganic route) and 362-378 m^2/g (organic route).
- TEM images confirm the presence of agglomerates and particles of varying sizes within the structure.

Article Info

Received: 23 Jul 2024
Accepted: 11 Aug 2025

Keywords

Sol-gel
Mesoporous γ-alumina
Structural properties

Abstract

This paper presents a comparative study of mesoporous γ-alumina preparation using organic and inorganic sol-gel processes. Aluminum chloride and aluminum isopropoxide (AIP) served as aluminum sources for the inorganic and organic routes, respectively. In the inorganic method, aluminum chloride was hydrolyzed with ammonium hydroxide at various hydrolysis ratios (10, 21, 31, 41, 52, 62). For the organic route, AIP was hydrolyzed at 85 °C with hydrolysis ratios ranging from 9 to 200 (mol H_2O/mol AIP) for comparison. A parametric study was conducted to analyze the effects of initial precursor concentration, hydrolysis ratio, and nitric acid to AIP ratio in the organic route. Physical characterization and phase evaluation of the γ-alumina samples were conducted using XRD, N_2-Physisorption, and TEM. The BET surface areas of the mesoporous γ-alumina materials ranged from 209 to 299 m^2/g for the inorganic method, and 362 to 378 m^2/g for the organic method. The mean pore diameter of the γ-alumina powders was approximately twice as large in the inorganic method compared to the organic method, with values of 8.9 nm and 4.8 nm, respectively. Optimal sol-gel process parameters for the organic method were identified as an initial AIP concentration of 0.1 M, a hydrolysis ratio of 150, and a nitric acid to AIP ratio of 0.3. The inorganic sol-gel method, which is cost-effective and easy to handle, produced results comparable to those reported in the literature.

1. INTRODUCTION

In recent years, mesoporous γ-alumina catalyst supports have attracted considerable attention due to their high specific surface area (SSA), pore volume (V_p), and porous architecture, particularly in petroleum refining and petrochemical processes [1,2]. This interest is due to their excellent thermal and mechanical stability, which makes them valuable in both industrial and academic applications involving catalytic reactions, adsorption, and separation [3–5]. The mesoporous structure, with sufficiently large pore diameters, mitigates diffusion limitations in catalytic reactions by enabling large molecules to access active catalyst sites [6]. Consequently, catalyst supports with wide pores and high SSA are essential for achieving efficient conversion of reactants into products. Among various metal oxides, mesoporous γ-alumina is widely used as a metal catalyst carrier due to its high SSA and acid/base centers, making it suitable for diverse industrial catalytic applications [7,8]. Controlled pore size distribution in alumina is particularly important for processing large molecules in catalytic reactions [9]. A variety of synthesis techniques, including precipitation, hydrothermal treatment, combustion, chemical vapor deposition, and sol-gel processing, have been developed to produce alumina powders [10,11]. Among these, the sol-gel method is especially effective for synthesizing metal oxides such as mesoporous γ-alumina because it enables precise control over SSA and pore size distribution [12]. This method involves a series of hydrolysis and condensation reactions, typically performed at low temperatures. Metal alkoxides are commonly employed

*Corresponding author, e-mail: orhan.ozcan@kocaeli.edu.tr

in sol-gel chemistry to form metal oxide clusters [13,14]. For example, hydrolysis of aluminum isopropoxide (AIP), a well-studied organic precursor, yields aluminum hydroxide, as shown in Equation (1):

$$Al(OR)_3 + 3H_2O \rightarrow Al(OH)_3OH + 3ROH, \qquad R = C_3H_7. \tag{1}$$

Although organic aluminum precursors such as AIP are widely used, they are associated with high costs, moisture sensitivity, and health hazards [15–18]. For this reason, inorganic aluminum precursors, such as aluminum chloride, are desirable for preparing γ-alumina powders. In the inorganic route, $AlCl_3$ reacts with ethanol to form chloroalkoxide complexes [19], as described in Equation (2):

$$AlCl_n + xC_2H_5OH \rightarrow Al(-OC_2H_5)_XCl_{n-x} + xHCl\,. \tag{2}$$

When sufficient ethanol is added, chloride-free modified metal alkoxides are obtained, which can then undergo hydrolysis in a basic medium through the addition of NH_4OH in varying amounts. The formation of oxo-bridges (M-OR) in the alcoholysis reaction of metal chlorides with alcohol is referred to as the nonhydrolytic route [20]. In this pathway, oxygen donors other than water in organic solvents form oxo-bridges, and condensation between alkoxides or between an alkoxide and a hydrolyzed alkoxide creates an inorganic network [21].

Despite extensive research, most studies have relied on AIP and aluminum sec-butoxide as precursors in the organic route [22–30], and to the best of our knowledge, direct comparative studies of organic versus inorganic sol-gel synthesis routes for γ-alumina remain absent in the literature. To address this gap, this work aims to prepare high SSA γ-alumina powders with mesoporous structures using two distinct sol-gel routes: one based on an organic precursor (AIP) and the other on an inorganic precursor (aluminum chloride). Additionally, a parametric study was conducted within the organic route to investigate how preparation conditions influence the physicochemical properties of γ-alumina powders. Comparing these two precursor systems is significant due to the preparation of high SSA alumina materials is of broad interest due to their applications in ceramics, adsorption, and catalysis. In addition, the sol-gel process has proven highly effective for producing mesoporous and nanocrystalline alumina with tailored properties. While organic precursors such as AIP offer high reactivity and controllable hydrolysis-condensation behavior, inorganic salts like aluminum chloride and aluminum nitrate provide cost-effective and environmentally benign alternatives. In these inorganic systems, precipitation and gelation depend on parameters such as pH, reagent addition sequence, and peptization, enabling the formation of samples with high SSAs and pore volumes. Furthermore, advanced techniques, such as ultrasonic-assisted sol formation, supercritical drying, and evaporation-induced self-assembly (EISA), have further improved structural integrity and porosity.

Evidence from prior studies highlights these points. Marinkovic et al. [31] synthesized nanocrystalline Al_2O_3 powders (315.18 m^2/g) via three wet-chemical methods, hydrothermal, reflux, and modified sol-gel, using AIP. The salt solution, prepared in isopropyl alcohol at 50 °C in an ultrasonic bath, was combined dropwise with a water/isopropanol mixture under continuous stirring. The pH was set to 12 using 0.1 M NaOH in all cases. The resulting gels were filtered, washed with a 1:1 (v/v) mixture of DI water and isopropanol, dried at 120 °C for 3 h, and calcined at 550 °C for 3 h. Wu et al. [32] reported that mesoporous alumina samples prepared using a soft template-assisted sol-gel process exhibited SSAs of 220-296 m^2/g. They used AIP as the precursor and F127 as the soft template. Mesoporous alumina (MA) was synthesized via two pathways: an aqueous-phase method using water or water-ethanol mixtures, and EISA method using pure alcohols. AIP was dissolved in 40 mL of solvent, prior to the addition of HNO_3 and F127. The solution was stirred, dried at 70 °C, and calcined at 700 °C. Seah et al. [33] developed a block copolymer-templated sol-gel technique to prepare mesoporous alumina (Al_2O_3), achieving a high surface area of 305 m^2/g and a pore volume of 0.33 cm^3/g. The method combined Pluronic F127, aluminum tri-sec-butoxide, ethanol, n-butanol, and nitric acid using EISA. In a two-step process, aluminum tri-sec-butoxide underwent controlled alcoholysis and hydrolysis with HNO_3 to form stable Al_2O_3 sols, which were then mixed with F127 to co-assemble into hybrid monoliths. The HNO_3/Al ratio significantly influenced mesophase formation. Solvent choice also affected the outcome by replacing ethanol with n-butanol slowed hydrolysis

and condensation, yielding hexagonal Al_2O_3 that produced a trimodal pore structure after calcination, with enhanced SSA and V_p. Thermal treatment up to 900 °C yielded crystalline γ-Al_2O_3 monoliths that retained mesostructural order. Yao et al. [34] synthesized γ-alumina with SSA values of 158-265 m^2/g from an inorganic aluminum nitrate solution. Aluminum hydroxide was precipitated by adding dilute ammonium hydroxide to an aqueous aluminum nitrate solution, raising the pH to approximately 9.2. Nitric acid was then added to the solution to reach a defined $[H^+]/[Al^{3+}]$ molar ratio, initiating peptization and promoting the formation of desired species. Ultrasonic treatment in a water bath facilitated the formation of a clear, stable alumina sol at ambient temperature. The sol was stirred for an extended period, vacuum-dried, and calcined at 350 °C, 450 °C, and 550 °C to yield alumina materials. Bauman et al. employed hydrated inorganic aluminum precursors, $AlCl_3.6H_2O$ and $Al(NO_3)_3.9H_2O$, to synthesize high-SSA alumina aerogels without alkoxide precursors, using a sol-gel method with propylene oxide as the gelation initiator [35]. The salts were dissolved in water, ethanol, or a 1:1 mixture of both. Propylene oxide initiated gelation, followed by ambient setting and ethanol solvent exchange. The gels were dried via supercritical CO_2 extraction, producing low-density, monolithic aerogels with morphologies dependent on the salt and solvent used. Calcination at 800 °C was conducted to evaluate structural transformations and thermal stability. Niero et al. [36] also used aluminum chloride and aluminum nitrate precursors to synthesize nanosized α-alumina. Reaction stoichiometry was optimized through solubility tests to maximize aluminum hydroxide ($Al(OH)_3$) yield and minimize byproducts such as NaCl and $NaNO_3$ by varying the reagent addition order and NaOH concentration. Reactions were conducted at 60 °C in a three-inlet reactor, with aluminum salts added dropwise to heated NaOH solution under constant stirring. After aging for 24 h, precipitates were centrifuged, washed, dried at 100 °C, and calcined at 1200 °C for 1 h. Xu et al. [37] prepared γ-alumina with a V_p of 5.4 cm^3/g, an SSA of 423.7 m^2/g, and a pore size of 37.8 nm after calcination at 500 °C, using various inorganic aluminum salts ($Al_3(SO_4)_2$, $AlCl_3$, and $Al(NO_3)_3$). γ-Al_2O_3 was synthesized through a controlled co-precipitation. A syringe pump regulated the addition of acidic aluminum solutions to alkaline NaOH, or acidic HNO_3 to alkaline $NaAlO_2$, maintaining a final pH of nearly 8.67. The resulting gel was aged for 48 h, washed with ethanol and distilled water, and dried using supercritical CO_2 (60 °C, 15 MPa) to preserve porosity. Calcination at 500 °C for 2 h yielded γ-Al_2O_3. Alves et. al. [38] explored the influence of pH on the morphology of alumina prepared via a sol-gel method using aluminum chloride hexahydrate as the precursor. The compound was hydrolyzed to form gelatinous aluminum hydroxide precipitate by adjusting the pH to 7. After aging for 24 h, the precipitate was filtered and washed to remove contaminants and moisture. Peptization was carried out using glacial acetic acid at 60-70 °C, maintaining a pH of approximately 3 to yield a clear, homogeneous sol. This sol was divided into three groups, acidic (3.0-4.5), neutral (6.0-7.0), and basic (8.0-9.0), to assess pH effects on gel formation.

These studies highlight the critical role of precursor chemistry and process conditions in determining final properties of alumina. It is also noteworthy that the physicochemical characteristics of γ-alumina are affected by preparation conditions and the type of initial precursors [39,40]. Therefore, this study evaluates a comparative evaluation of organic and inorganic sol-gel routes for γ-alumina synthesis. Using X-ray diffraction (XRD), N_2 physisorption, and transmission electron microscopy (TEM), we characterize and compare the structural and textural properties of the resulting powders, thereby investigating the influence of precursor type and synthesis conditions on the textural properties of the sol-gel prepared materials.

2. MATERIAL METHOD

This study aimed to synthesize and characterize a family of γ-alumina powders prepared via the sol-gel method through both organic and inorganic routes. The choice of the sol-gel method was based on its proven ability to produce high-purity, nanostructured materials with controlled porosity. The comparative investigation between the two synthesis routes was intended to understand how variations in precursor salts and hydrolysis conditions affect the structural and textural properties of resulting powders.

2.1. Materials

In the organic route, the following reagents were employed: aluminum isopropoxide, $Al(OC_3H_7)_3$ (AIP, ≥98%, Sigma-Aldrich Chemie GmbH), 1-propanol (≥99.5%, Merck), and nitric acid (65%, Merck). In the inorganic route, the reagents included aluminum chloride ($AlCl_3$, ≥98%, Merck), ethanol (≥99.9%, Merck),

and ammonia solution (25%, Merck). Commercial γ-alumina powders (SASOL, Siralox 1.5/100) were used as a reference material (ref-Al) for comparing the properties of the prepared sol-gel samples. All reagents were used without further purification. Deionized water (DI) was employed in all the experimental procedures.

2.2. Sol-gel Preparation Procedures

For the organic route, a measured quantity (0.02 mol) of AIP was dissolved in 1-propanol under ambient conditions to create a homogeneous solution suitable for hydrolyzing the alkoxide structure. The mixture was heated to 85 ℃ under magnetic stirring. Deionized water was then added at specific molar ratios (R=mol H_2O/mol AIP, ranging from 9 to 31) to initiate hydrolysis. For the condensation step, nitric acid was introduced at a fixed molar ratio of 0.1 (mol HNO_3/mol AIP), and the mixture was stirred vigorously for 6 h. Additional experiments were conducted to evaluate the effects of initial AIP concentration (0.1 M, 0.3 M, 0.5 M), hydrolysis ratio (R = 100, 150, 200), nitric acid-to-AIP molar ratio (0.1, 0.3, 0.5). These parameters were selected based on previous studies showing that low hydrolysis ratios yield powders with larger pore diameters and higher specific surface areas (SSA), while higher ratios result in smaller pore diameters and lower SSA [28]. The chosen AIP concentrations enabled assessment of sol density effects on particle agglomeration and porosity [41], while variations in nitric acid concentration provided insights into acid-catalyzed influences on condensation rate and phase evolution [42].

For the inorganic route, 0.02 mol of $AlCl_3$ was dissolved in ethanol at room temperature to form chloroalkoxide complexes [19]. Ammonium hydroxide (NH_4OH, 25%) was then added at hydrolysis ratios of 10, 21, 31, 41, 52, and 62, initiating hydrolysis in a basic medium. This promoted condensation and gel formation.

The resulting gels were aged for two days at room temperature, after which the solvent was removed using a rotary evaporator under vacuum at 60 ℃ for 30 min. The gels were subsequently dried in an oven at 100 ℃ for 24 h in a stagnant atmosphere, and calcined at 500 ℃ for 3 h to yield mesoporous γ-alumina [43].

Table 1 presents an overview of all the materials prepared via organic and inorganic sol-gel routes, detailing hydrolysis ratio, temperature, solvent, and synthesis route. In the organic route, AIP was hydrolyzed with water at different hydrolysis ratios (R = 9, 11, 13, 15, 21, 31) to compare the textural properties with those of the mesoporous γ-alumina samples prepared using the inorganic route, where NH_4OH was used for hydrolysis.

Table 1. *γ-alumina powders prepared in the organic and inorganic sol-gel processes*

Material name	Hydrolysis ratio (R)	Hydrolysis temperature (℃)	Alcohol type	Sol-gel route
Al-R9	9	85	1-propanol	Organic
Al-R11	11	85	1-propanol	Organic
Al-R13	13	85	1-propanol	Organic
Al-R15	15	85	1-propanol	Organic
Al-R21	21	85	1-propanol	Organic
Al-R31	31	85	1-propanol	Organic
Al-10	10	25	Ethanol	Inorganic
Al-21	21	25	Ethanol	Inorganic
Al-31	31	25	Ethanol	Inorganic
Al-41	41	25	Ethanol	Inorganic
Al-52	52	25	Ethanol	Inorganic
Al-62	62	25	Ethanol	Inorganic

Furthermore, an additional parametric study was conducted in the organic route by varying the initial AIP concentration, hydrolysis ratio, and nitric acid/AIP molar ratio to observe their effects on textural and

structural properties. Nitric acid was used to lower the pH of the solution, thereby maintaining the hydrolysis and condensation reaction rates. This is due to the fact that the acid-catalyzed sol-gel process promotes the formation of linear structures by replacing OR groups with OH groups. In contrast, the inorganic route, conducted in a basic medium, produces more compact, dense structures [44]. Additional sol-gel process parameter variations are summarized in Table 2, which specifies the initial AIP concentrations, hydrolysis ratios, and nitric acid-to-AIP molar ratios tested.

Table 2. *Range of parameters to prepare γ-alumina powders in the organic route*

Material name	Initial Concentration (M)	Hydrolysis ratio (R)	HNO_3/AIP molar ratio
Al_0.1M	0.1	100	0.1
Al_0.3M	0.3	100	0.1
Al_0.5M	0.5	100	0.1
Al_R150	0.1	150	0.1
Al_R200	0.1	200	0.1
Al_0.3N	0.1	150	0.3
Al_0.5N	0.1	150	0.5

2.3. Characterization

Powder X-ray diffraction (XRD) patterns of calcined samples were obtained using a Rigaku MiniFlex diffractometer with CuKα radiation (λ=0.154 nm) at a scanning rate of 2°/min over a 2θ range of 10°-80° scanning angles. Average crystallite size was determined using the Debye-Scherrer method (Equation (3)), based on the full width at half-maximum (FWHM) of the XRD peaks

$$D = 0.9\lambda/\beta \cos\theta \,. \quad (3)$$

N_2 adsorption-desorption isotherms were recorded using a Micromeritics ASAP 2020 instrument with the sample held at its normal boiling point (at 101 kPa). Prior to measurements, samples were subjected to an outgassing process under vacuum at 200 °C for a period of 2 h. The SSA and BJH pore size distribution were determined using the BET and BJH models, respectively. Transmission electron microscopy (TEM) images were acquired using a JEOL JEM 2100 high-resolution transmission electron microscope (HRTEM) at 200 kV to examine the morphology of the samples.

3. THE RESEARCH FINDINGS AND DISCUSSION

3.1. Comparison of Textural Properties

Table 3 presents the textural properties of γ-alumina materials prepared via sol-gel methods using both organic and inorganic routes with varying hydrolysis ratios.

Table 3. *Textural properties of organic and inorganic route samples*

Material name	BET surface area (m^2/g)	BJH desorption pore volume (cm^3/g)	BJH desorption average pore diameter (nm)
ref-Al	108	0.4	9.6
Al-10	231	0.4	4.4
Al-21	299	1.0	9.1
Al-31	297	0.9	8.7
Al-41	236	0.4	4.6
Al-52	217	0.4	4.6
Al-62	209	0.3	4.3

Al-R9	372	0.8	4.9
Al-R11	378	1.0	4.9
Al-R13	376	0.9	4.9
Al-R15	369	0.9	5.3
Al-R21	362	0.9	4.8
Al-R31	369	0.9	4.9

For the inorganic-route samples, the highest BET surface areas (297-299 m^2/g) were obtained at hydrolysis ratios of 21 and 31 (Figure 1). In this route, the BET surface area increased with hydrolysis ratio up to Al-21 and Al-31, after which it declined. This trend can be attributed to the effect of pH and hydroxyl ion concentration on the sol-gel network structure. According to Sharma et al. [45], increasing pH (or equivalently, increasing base addition such as NH_4OH) beyond a certain point leads to larger α-Al_2O_3 particle sizes (up to 750 nm at pH 12) due to uncontrolled hydrolysis and condensation reactions, leading to highly branched polymeric structures and particle agglomeration. As particle size increases, surface area decreases, given the inverse relationship between the two parameters [46]. Al-21 and Al-31 were selected for comparison with the organic route materials due to their high BET surface areas (297-299 m^2/g) and relatively large pore diameter (8.7-9.1 nm), along with commercial γ-alumina (ref-Al). According to the International Union of Pure and Applied Chemistry (IUPAC) [18], pores with diameters between 2 and 50 nm are classified as mesopores. The inorganic-route alumina samples exhibited mesoporosity, with pore diameters ranging from 4.3 to 9.6 nm, as confirmed by their adsorption-desorption isotherms (Figure 2). The isotherms corresponded to type IV in the Brunauer-Deming-Deming-Teller (BDDT) classification system, indicating mesoporosity and strong interaction between the solid surfaces. Based on IUPAC classification, ref-Al exhibited an H2-type hysteresis loop, characterized by an almost flat plateau at high p/p^o, suggesting complex pore networks with varied sizes and shapes. In contrast, Al-21 and Al-31 displayed H3-type hysteresis loops, indicating non-rigid pore structures due to the absence of a plateau at high p/p^o, consistent with the behavior of non-rigid flat and plate-like particles, as previously reported elsewhere [41]. Figure 3 shows the pore volume distributions of Al-21 and Al-31 at the mesoporous scale. Both samples exhibited larger pore volumes than ref-Al. Their adsorption-desorption isotherms demonstrated indicated significantly higher adsorbed gas volumes (600 cm^3/g STP) compared to ref-Al (250 cm^3/g STP). The narrow pore volume distributions (Figure 3) suggest the presence of uniform pores in all samples, with an average pore diameter of approximately 14 nm [22].

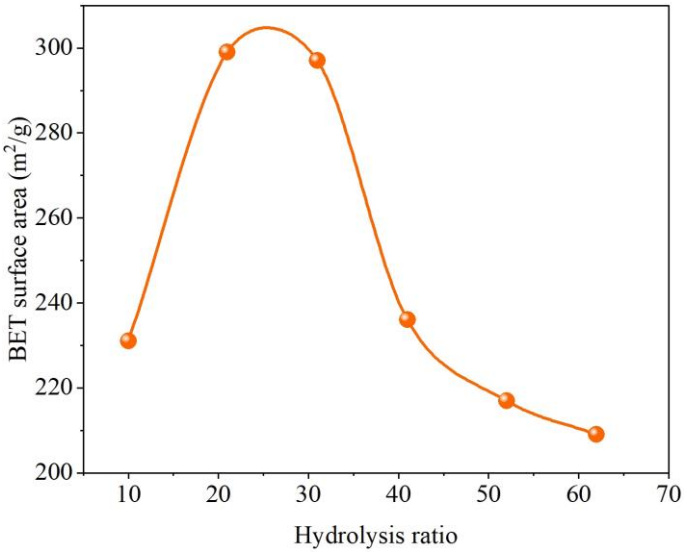


Figure 1. *BET surface area with increasing hydrolysis ratio in inorganic route*

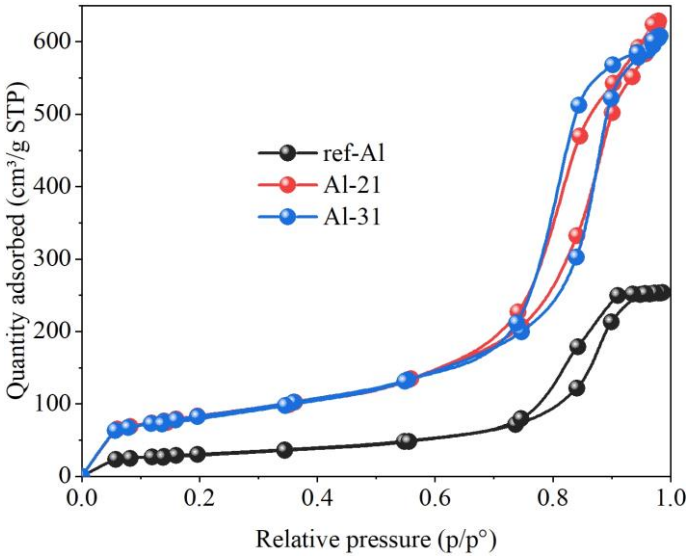


Figure 2. *Adsorption-desorption isotherms of ref-Al, Al-21, and Al-31*

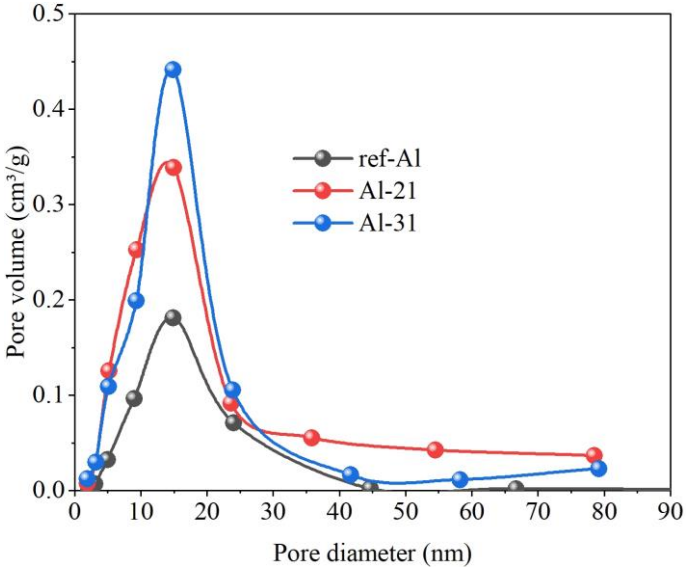


Figure 3. *Pore volume distribution of ref-Al, Al-21, and Al-31*

The γ-alumina samples produced via the organic sol-gel process exhibited BET surface areas ranging from 362 to 378 m^2/g and average pore diameters from 4.8 to 5.3 nm. A comparison was made between organic-route samples (Al-R21, Al-R31) and inorganic-route samples (Al-21, Al-31), given their similar hydrolysis ratios during preparation (Table 1). Table 3 presents the textural properties of these samples. The BJH desorption average pore diameters were 4.8 nm for the organic-route samples and 8.9 nm for the inorganic route samples. Although, Al-21 and Al-31 exhibited lower BET surface areas, their pore diameters were larger than Al-R21 and Al-R31. The higher BET surface areas observed of the organic-route samples may be attributed to the increased stability of colloids derived from organic salts during synthesis, as previously reported in [44]. Colloids formed through the hydrolysis of metal alkoxide solutions generally exhibit greater stability compared to those derived from aqueous inorganic salt solutions, due to the absence of destabilizing anions [44]. Organic precursors such as aluminum isopropoxide hydrolyze in a controlled manner [24] under acidic conditions [47], promoting the formation of stable colloidal dispersions, resulting in high surface areas and relatively narrow pore size distribution [48]. Figures 4 and 5 present the adsorption-desorption isotherms and pore volume distributions of the organic and inorganic-route powders in comparison with ref-Al.

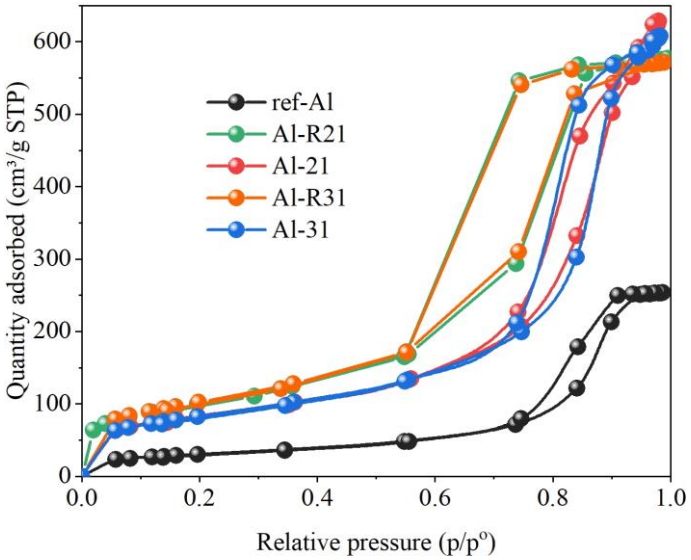


Figure 4. *Adsorption-desorption isotherms of selected organic and inorganic samples with ref-Al.*

All samples exhibited type IV isotherms with a mixture of H2 and H3 hysteresis loops, indicating the presence of different pore shapes. Transitioning from an organic salt precursor (H2 hysteresis) to an inorganic salt precursor (H3 hysteresis) led to a shift in pore shape from disordered ink-bottle (narrow neck) structures with complex networks to plate-like particles [49,50]. The pore volume distributions for materials synthesized via both routes fell within the mesoporous range. Furthermore, the average pore diameters of Al-R21 and Al-R31 were closer to the microporous region than those of Al-21 and Al-31.

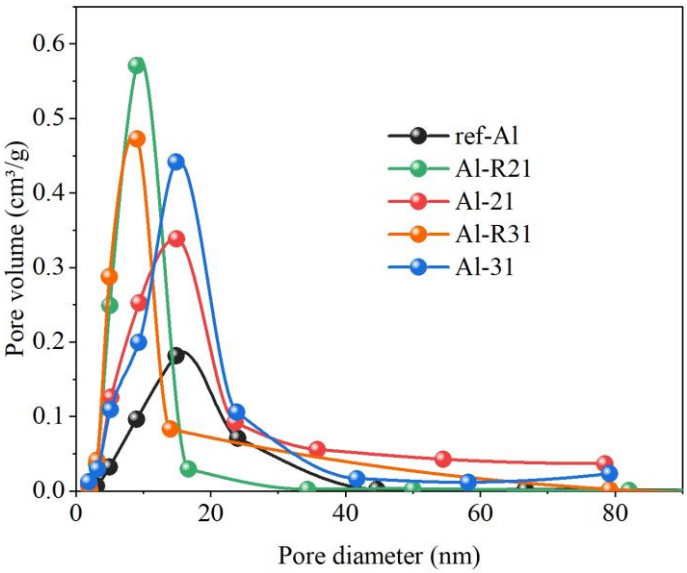


Figure 5. *Pore volume distributions of selected organic and inorganic samples with ref-Al*

3.2. Comparison of the Structural Properties and Morphology

Figure 6 depicts the XRD patterns of all calcined samples prepared via the inorganic route in comparison with ref-Al. As illustrated in the figure, the crystallinity of all synthesized materials was notably lower than that of ref-Al. All materials exhibited characteristic γ-alumina diffraction peaks at 2θ values of 37°, 47°, and 67° (JCPDS 29-0063). The peak intensities remained nearly constant across the inorganic-route samples as the hydrolysis ratio increased, indicating similar crystallite sizes.

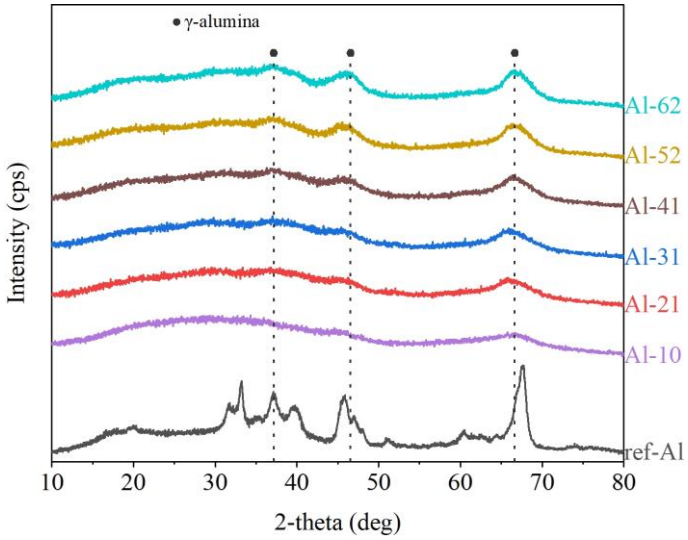


Figure 6. *XRD patterns of samples in inorganic route*

Table 4 presents the average crystalline sizes of ref-Al, Al-21, Al-31, and the organic route samples, calculated using the Scherrer equation. The crystalline size of ref-Al was larger than that of the other samples, due to the presence of a characteristic peak with high intensity. In contrast, both organic and inorganic-route samples exhibited similar, smaller crystallite sizes in the range of 1-2 nm.

Table 4. *Scherrer average crystalline sizes*

Material name	Crystalline size (nm)
ref-Al	6.5
Al-21	1.1
Al-R21	1.8
Al-31	1.6
Al-R31	1.8

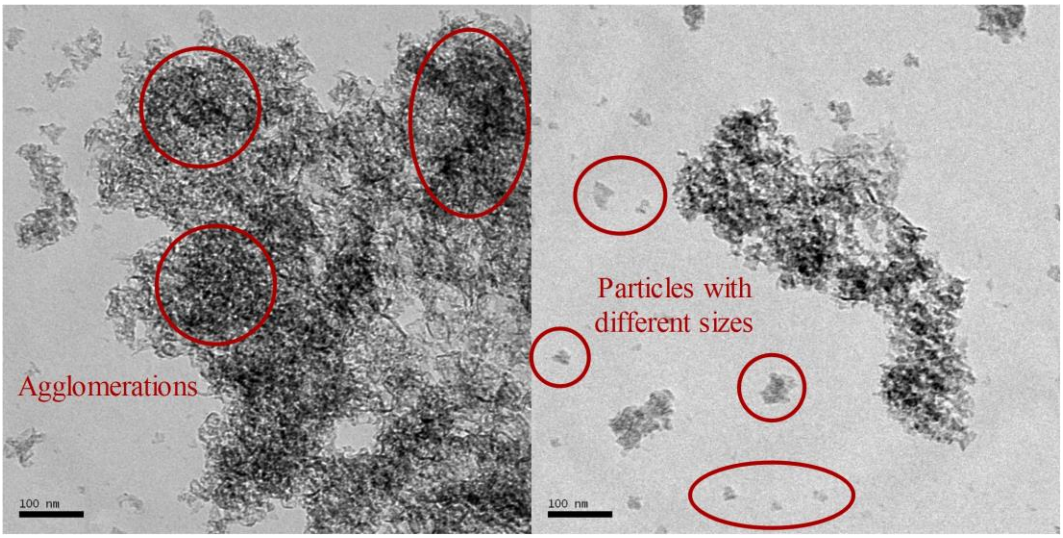


Figure 7. *TEM images of Al-21*

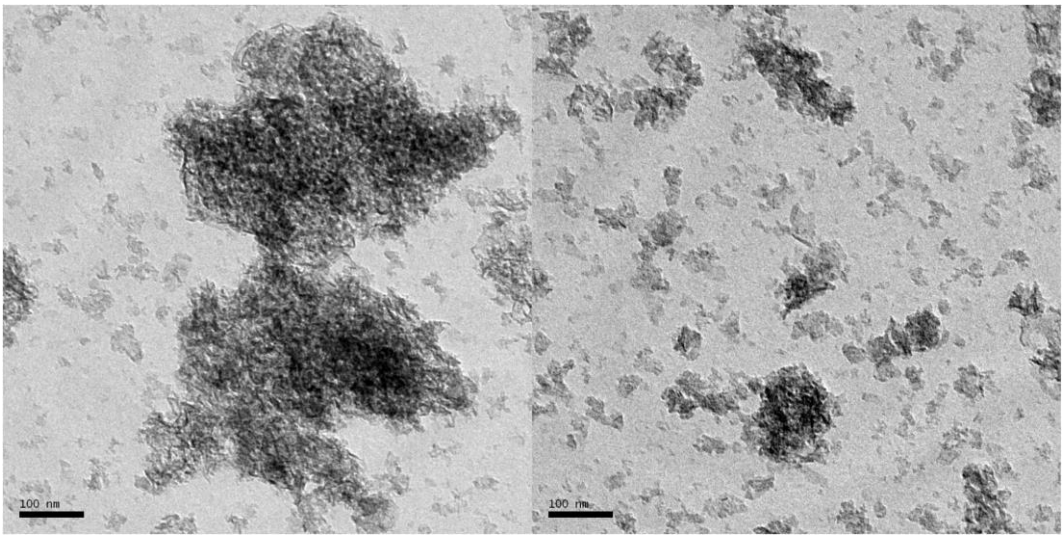


Figure 8. *TEM images of Al-31*

Figures 7 and 8 present transmission electron micrographs of Al-21 and Al-31, respectively. The images reveal agglomerated particles on the left and nanoparticles adjacent to these agglomerates on the right. Compared with the organic-route samples, Al-21 and Al-31 exhibit larger agglomerates and more particle groupings, indicating a denser structure. These observations are consistent with the differences in BET surface areas and pore size distributions. Figure 9 displays the XRD patterns of organic-route samples (Al-R21 and Al-R31) and inorganic-route samples (Al-21 and Al-31) in comparison with the reference sample (ref-Al). Both organic and inorganic-route samples exhibit broader and less intense diffraction peaks than ref-Al, indicating smaller crystallite sizes and lower crystallinity, in agreement with the Scherrer-based size calculations. Furthermore, the organic-route samples show peak intensities comparable to those of their inorganic-route counterparts, suggesting similar crystallite sizes. Figures 10 and 11 present the TEM images of the organic-route samples Al-R21 and Al-R31, respectively. As previously noted, these samples display disordered, linear particles characteristic of the acid-catalyzed sol-gel technique used in their preparation. The loosely connected linear morphology observed in both samples suggests limited aggregation.

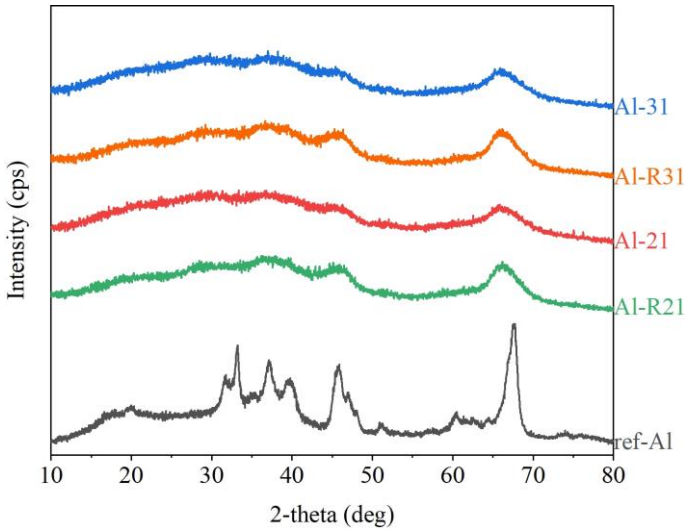


Figure 9. *XRD patterns of the selected samples*

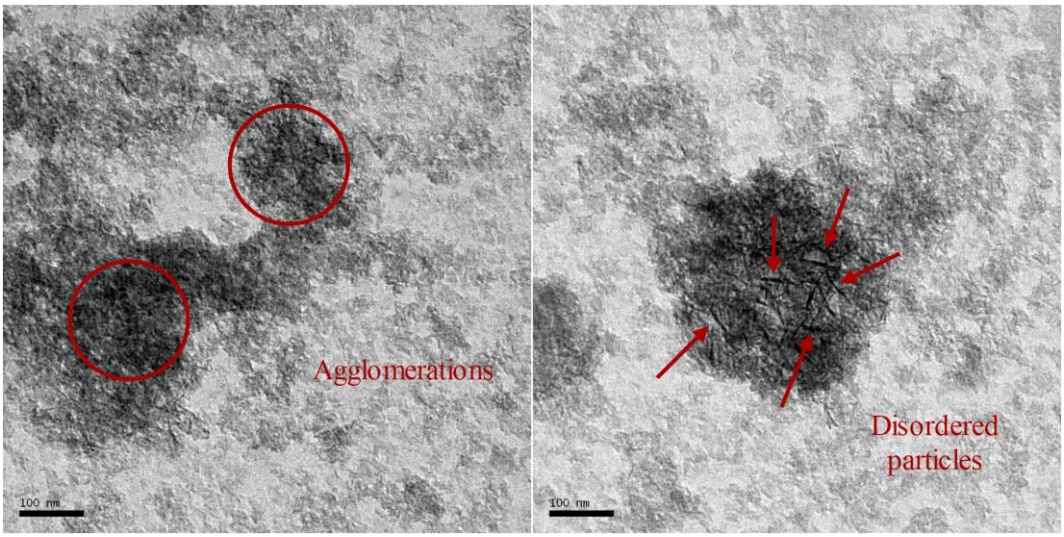


Figure 10. *TEM micrographs of Al-R21*

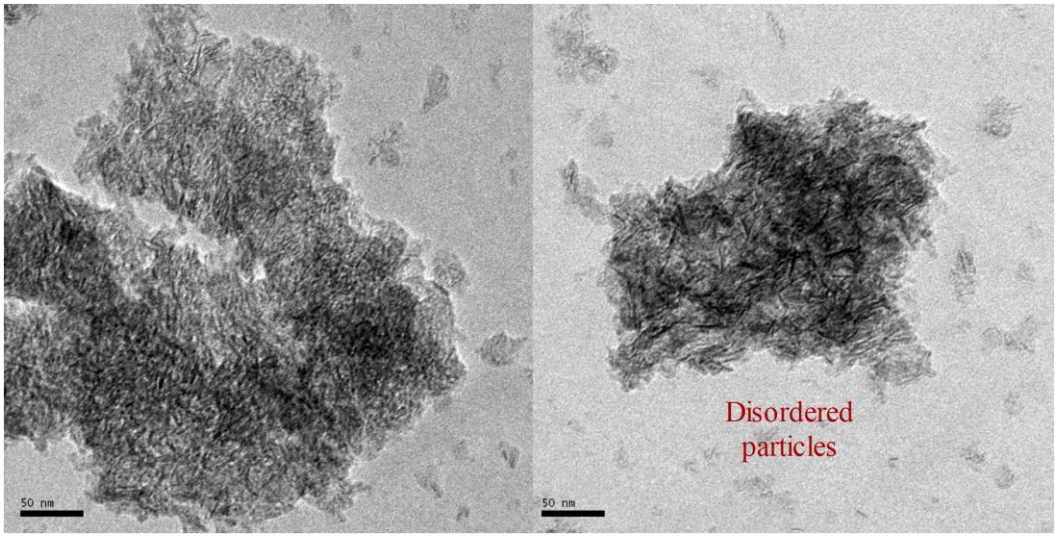


Figure 11. *TEM micrographs of Al-R31*

3.3. Parametric Study in the Organic Route

Certain process parameters are crucial in the organic sol-gel method, including the hydrolysis ratio (mol H_2O/mol AIP), the initial AIP concentration (mol/L), and the nitric acid to AIP ratio (mol HNO_3/mol AIP) during preparation [41]. The parametric study focused exclusively on the organic route due to the higher BET surface areas obtained. Table 5 summarizes the materials and their corresponding textural properties. Figure 12 illustrates the influence of sol-gel process parameters on BET surface area, BJH desorption pore volume, and BJH desorption average pore diameter in panels a-c. As shown in Figure 12a, all parameters followed a similar trend with increasing hydrolysis ratio. However, more complex effects on the textural properties were observed when varying the initial precursor concentration (Figure 12b) and the nitric acid to AIP ratio (Figure 12c). It can be concluded that the hydrolysis ratio significantly impacts all parameters due to its role as the primary reaction in the preparation process. In contrast, the sol-to-gel transformation process is primarily influenced by the initial concentration and HNO_3/AIP ratio [51]. Consequently, the gelation rate displays a complex behavior, consistent with previous reports [26,41], thereby supporting our findings.

Table 5. *Conditions of the parametric study*

Designation	Al_0.1M	Al_0.3M	Al_0.5M	Al_R150	Al_R200	Al_0.3N	Al_0.5N
Initial concentration	0.1	0.3	0.5	0.1	0.1	0.1	0.1
Hydrolysis ratio	100	100	100	150	200	150	150
Nitric acid to AIP ratio	0.1	0.1	0.1	0.1	0.1	0.3	0.5
BET surface area (m^2/g)	277	272	266	349	308	369	343
BJH desorption pore volume (cm^3/g)	0.3	0.3	0.3	0.8	0.5	0.8	0.8
BJH desorption average pore diameter (nm)	2.9	2.8	2.8	5.2	4.3	4.9	6.6

The optimal sol-gel process parameters, determined from the results in Figure 12, were an initial AIP concentration of 0.1 M, a hydrolysis ratio of 150, and a nitric acid to AIP ratio of 0.3. The sample synthesized under these conditions was designated as Al_0.3N.

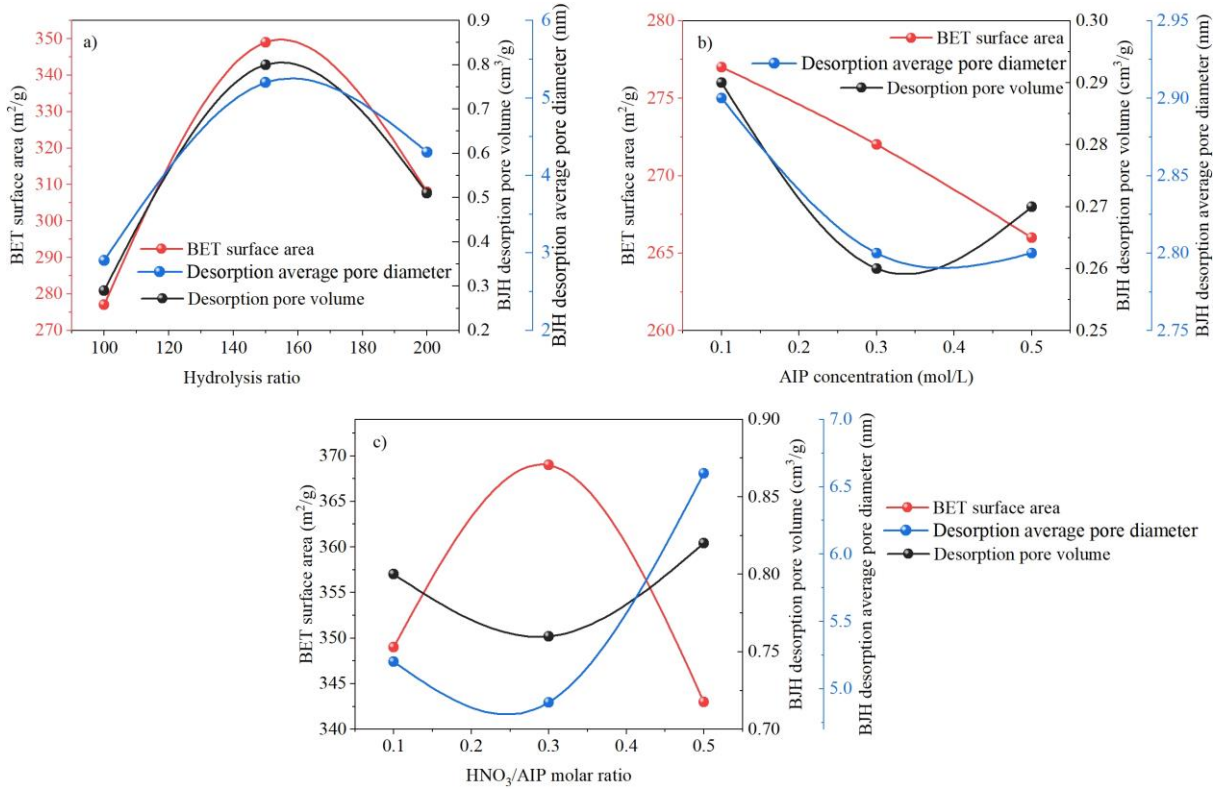


Figure 12. *Effects of (a) hydrolysis ratio, (b) initial concentration, and (c) HNO_3/AIP ratio on BET surface area, BJH desorption pore volume, and BJH desorption average pore diameter*

4. RESULTS

In the present study, γ-Al_2O_3 powders were synthesized using two different initial precursors, aluminum chloride ($AlCl_3$) and aluminum isopropoxide (AIP). The samples were characterized by X-ray diffraction (XRD), N_2-Physisorption, and transmission electron microscopy (TEM) to evaluate the effects of precursor type on their textural, structural, and morphological properties. The inorganic route involved the sol-gel synthesis of γ-alumina powders at room temperature using an ethanolic solution of $AlCl_3$. The BET surface areas ranged from 209-299 m^2/g for the inorganic route and 362-378 m^2/g for the organic route. The highest SSA in the inorganic route was achieved at hydrolysis ratios of 21 and 31. XRD anaysis showed that all γ-alumina samples from both sol-gel methods indicated average crystalline sizes in the range of 1-2 nm. TEM images of both organic and inorganic-route samples revealed agglomerates and γ-alumina particles of varying sizes. The average BJH desorption pore diameter was larger for inorganic route samples (8.9 nm) than for organic-route samples (4.8 nm). The optimal sol-gel process parameters were determined to be an initial AIP concentration of 0.1 M, a hydrolysis ratio of 150, and a nitric acid to AIP ratio of 0.3. The BET surface areas obtained for the organic route (362-378 m^2/g) agree well with previous sol-gel studies using AIP and block-copolymer templates, which report SSAs up to 409-508 m^2/g with narrow pore size distributions [3,52]. Moreover, these values exceed those reported by Marinkovic et al. [31] (315 m^2/g) and Seah et al. [33] (305 m^2/g) for similar alkoxide-based sol-gel syntheses, demonstrating the effectiveness of the preparation conditions employed in this work. In contrast, γ-alumina prepared from inorganic salts under non-templated conditions typically yields lower SSAs (290-398 m^2/g), as observed for $AlCl_3$ hydrolyzed in the presence of NH_4OH at neutral pH [53]. The SSAs of our inorganic-route samples (209-299 m^2/g) are within the upper range of those reported by Yao et al. [34] (158-265 m^2/g), indicating that our method produces competitive textural properties.

ACKNOWLEDGEMENTS

This study was derived from a master's thesis titled "Preparation and Characterization of Mesoporous Nano-Alumina and CoMo/Al_2O_3 Catalysts by the Sol-Gel Method" in the Department of Chemical Engineering, Institute of Science, Kocaeli University.

CONFLICTS OF INTEREST

No conflict of interest was declared by the authors.

REFERENCES

[1] Xue, L., Wei, J., Zhang, D., Li, X., Liu, X., "Tuning the structure of alumina", Journal of Porous Materials, 22: 1119–1126, (2015).

[2] Said, S., Abdelrahman, A.A., "Atomic layer deposition of MoO_3 on mesoporous γ-Al_2O_3 prepared by sol–gel method as efficient catalyst for oxidative desulfurization of refractory dibenzothiophene compound", Journal of Sol-Gel Science and Technology, 95: 308–320, (2020).

[3] Wu, W., Wan, Z., Chen, W., Zhu, M., Zhang, D., "Synthesis of mesoporous alumina with tunable structural properties", Microporous and Mesoporous Materials, 217: 12–20, (2015).

[4] Mendoza Hernández, J.C., Pérez Osorio, G., Gutiérrez Arias, J.E.M., Castañeda Camacho, J., "Degradation of dye containing in textile wastewater by sequential process: photocatalytic and biological treatment", Turkish Journal of Chemistry, 46:2046–2056, (2022).

[5] Lakade, S.H., Harde, M.T., Deshmukh, P.K., "Synthesis of mesoporous alumina: an impact of surface chemistry on release behavior", Particulate Science and Technology, 38: 1035–1041, (2020).

[6] Han, D., Li, X., Zhang, L., Wang, Y., Yan, Z., Liu, S., "Hierarchically ordered meso/macroporous γ-alumina for enhanced hydrodesulfurization performance", Microporous and Mesoporous Materials, 158: 1–6, (2012).

[7] Rutkowska, I., Marchewka, J., Jeleń, P., Odziomek, M., Korpyś, M., Paczkowska, J., Sitarz,M., "Chemical and structural characterization of amorphous and crystalline alumina obtained by alternative sol-gel preparation routes", Materials, 14: 1761, (2021).

[8] Sobhani, M., Tavakoli, H., Chermahini, M.D., Kazazi, M., "Preparation of macro-mesoporous γ-alumina via biology gelatin assisted aqueous sol-gel process", Ceramics International, 45: 1385–1391, (2019).

[9] Ishihara, A., Tatebe, K., Hashimoto, T., Nasu, H., "Preparation of Silica, Alumina, Titania, and Zirconia with Different Pore Sizes Using Sol-Gel Method and Their Properties as Matrices in Catalytic Cracking", Industrial and Engineering Chemistry Research, 57: 14394–14405, (2018).

[10] Wu, G., Liu, G., Li, X., Peng, Z., Zhou, Q., Qi, T., "A green approach of preparation of fine active alumina with high specific surface area from sodium aluminate solution", RSC Advances, 9: 5628–5638, (2019).

[11] Tabesh, S., Davar, F., Loghman-Estarki, M.R., "Preparation of γ-Al_2O_3 nanoparticles using modified sol-gel method and its use for the adsorption of lead and cadmium ions", Journal of Alloys and Compounds, 730: 441–449, (2018).

[12] Cai, G., Zheng, X., Zheng, Y., Xiao, Y., Zheng, Y., "Synthesis of ordered mesoporous boron-doped γ-alumina with high surface area and large pore volume", Materials Letters, 178: 248–251, (2016).

[13] Al Khudhair, A., Bouchmella, K., Mutin, P.H., Hulea, V., Gimello, O., Mehdi, A., "Hydrolytic vs. Nonhydrolytic Sol-Gel in Preparation of Mixed Oxide Silica–Alumina Catalysts for Esterification", Molecules, 27: 2534, (2022).

[14] Yelten, A., Karal-Yilmaz, O., Akguner, Z.P., Bal-Ozturk, A., Yilmaz, S., "In-vitro bioactivity investigation of sol-gel derived alumina-bovine hydroxyapatite (Bha) composite powders", Gazi University Journal of Science, 33: 690–700, (2020).

[15] Teoh, G.L., Liew, K.Y., Mahmood, W.A.K., "Synthesis and characterization of sol-gel alumina nanofibers", Journal of Sol-Gel Science and Technology, 44: 177–186, (2007).

[16] Fu, Q., Cao, C.B., Zhu, H.S., "Preparation of alumina films from a new sol-gel route", Thin Solid Films, 348: 99–102, (1999).

[17] Caruso, R.A., Antonietti, M., "Sol-gel nanocoating: An approach to the preparation of structured materials", Chemistry of Materials, 13: 3272–3282, (2001).

[18] Gash, A.E., Tillotson, T.M., Satcher, J.H., Hrubesh, L.W., Simpson, R.L., "New sol-gel synthetic route to transition and main-group metal oxide aerogels using inorganic salt precursors", Journal of Non-Crystalline Solids, 285: 22–28, (2001).

[19] Sobhani, M., Sedaghat, A., Ebadzadeh, T., Ebrahimi, M., "Preparation of nano-sized $Mg_{0.6}Al_{0.8}Ti_{1.6}O_5$ powders using the inorganic salts route", Ceramics International, 39: 6899–6905, (2013).

[20] Mutin, P.H., Vioux, A., "Nonhydrolytic processing of oxide-based materials: Simple routes to control homogeneity, morphology, and nanostructure", Chemistry of Materials, 21: 582–596, (2009).

[21] Debecker, D.P., Hulea, V., Mutin, P.H., "Mesoporous mixed oxide catalysts via non-hydrolytic sol-gel: A review", Applied Catalysis A: General, 451: 192–206, (2013).

[22] Renuka, N.K., Shijina, A.V., Praveen, A.K., "Mesoporous γ-alumina nanoparticles: Synthesis, characterization and dye removal efficiency", Materials Letters, 82: 42–44, (2012).

[23] Rashidi, F., Kharat, A.N., Rashidi, A.M., Lima, E., Lara, V., Valente, J.S., "Fractal geometry approach to describe mesostructured boehmite and gamma-alumina nanorods", European Journal of Inorganic Chemistry, 1544–1551, (2010).

[24] Huang, B., Bartholomew, C.H., Woodfield, B.F., "Facile synthesis of mesoporous γ-alumina with tunable pore size: The effects of water to aluminum molar ratio in hydrolysis of aluminum alkoxides", Microporous and Mesoporous Materials, 183: 37–47, (2014).

[25] Bejenaru, N., Lancelot, C., Blanchard, P., Lamonier, C., Rouleau, L., Payen, E., Dumeignil, F., Royer, S., "Synthesis, characterization, and catalytic performances of novel CoMo hydrodesulfurization catalysts supported on mesoporous aluminas", Chemistry of Materials, 21: 522–533, (2009).

[26] Akia, M., Alavi, S.M., Rezaei, M., Yan, Z.F., "Optimizing the sol-gel parameters on the synthesis of mesostructure nanocrystalline γ-Al_2O_3", Microporous and Mesoporous Materials, 122: 72–78, (2009).

[27] Park, Y.K., Tadd, E.H., Zubris, M., Tannenbaum, R., "Size-controlled synthesis of alumina nanoparticles from aluminum alkoxides", Materials Research Bulletin, 40: 1506–1512, (2005).

[28] Dumeignil, F., Sato, K., Imamura, M., Matsubayashi, N., Payen, E., Shimada, H., "Modification of structural and acidic properties of sol-gel-prepared alumina powders by changing the hydrolysis ratio", Applied Catalysis A: General, 241: 319–329, (2003).

[29] Khaleel, A.A., Klabunde, K.J., "Characterization of aerogel prepared high-surface-area alumina: In situ FTIR study of dehydroxylation and pyridine adsorption", Chemistry - A European Journal, 8: 3991–3998, (2002).

[30] Pierre, A.C., Elaloui, E., Pajonk, G.M., "Comparison of the structure and porous texture of alumina gels synthesized by different methods", Langmuir, 14: 66–73, (1998).

[31] Marinković, M., Waisi, H., Blagojević, S., Zarubica, A., Ljupković, R., Krstić, A., Janković, B. Ž., "The effect of process parameters and catalyst support preparation methods on the catalytic efficiency in transesterification of sunflower oil over heterogeneous KI/Al_2O_3-based catalysts for biodiesel production", Fuel, 315, (2022).

[32] Wu, W., Zhu, M., Zhang, D., "The role of solvent preparation in soft template assisted synthesis of mesoporous alumina", Microporous and Mesoporous Materials, 260: 9–16, (2018).

[33] Seah, G.L., Wang, L., Tan, L.F., Tipjanrawee, C., Sasangka, W.A., Usadi, A.K., McConnachie, J. M., Tan, K.W., "Ordered Mesoporous Alumina with Tunable Morphologies and Pore Sizes for CO_2 Capture and Dye Separation", ACS Applied Materials and Interfaces, 13: 36117–129, (2021).

[34] Yao, N., Xiong, G., Zhang, Y., He, M., Yang, W., "Preparation of novel uniform mesoporous alumina catalysts by the sol-gel method", Catalysis Today, 68: 97–109, (2001).

[35] Baumann, T.F., Gash, A.E., Chinn, S.C., Sawvel, A.M., Maxwell, R.S., Satcher, J.H., "Synthesis of high-surface-area alumina aerogels without the use of alkoxide precursors", Chemistry of Materials, 17: 395–401, (2005).

[36] Niero, D.F., Montedo, O.R.K., Bernardin, A.M., "Synthesis and characterization of nano α-alumina by an inorganic sol–gel method", Materials Science and Engineering: B, 280: 115690, (2022).

[37] Xu, J., Ibrahim, A.R., Hu, X., Hong, Y., Su, Y., Wang, H., Li, J., "Preparation of large pore volume γ-alumina and its performance as catalyst support in phenol hydroxylation", Microporous and Mesoporous Materials, 231: 1–8, (2016).

[38] Alves, A.K., Berutti, F.A., Bergmann, C.P., "The effects of pH on the preparation of alumina by sol-gel process", Particulate Science and Technology, 23: 351–360, (2005).

[39] Li, L., Liu, X., Wang, G., Liu, Y., Kang, W., Deng, N., Zhuang, X., Zhou, X., "Research progress of ultrafine alumina fiber prepared by sol-gel method: A review", Chemical Engineering Journal, 421: 127744, (2021).

[40] Yi, H., Wan, Y., Zhang, Y., Wang, Y., Fei, W., Luo, G., "Controllable preparation of highly uniform γ-alumina microspheres via the sol–gel route for alkoxide in a coaxial microchannel", Journal of Sol-Gel Science and Technology, 93: 391–401, (2020).

[41] Kibar, M.E., Özcan, O., Dusova-Teke, Y., Yonel-Gumruk, E., Akin, A.N., "Optimization, modeling and characterization of sol-gel process parameters for the synthesis of nanostructured boron doped alumina catalyst supports", Microporous and Mesoporous Materials, 229: 134–144, (2016).

[42] Ciriminna, R., Fidalgo, A., Pandarus, V., Béland, F., Ilharco, L.M., Pagliaro, M., "The Sol–Gel Route to Advanced Silica-Based Materials and Recent Applications", Chemical Reviews, 113: 6592–6620, (2013).

[43] Kobayashi, Y., Yasuda, Y., Morita, T., "Low-temperature synthesis of α-alumina based on sol-gel processes", Advances in Materials and Processing Technologies, 7: 482–513, (2021).

[44] Turova, N.Y., Turevskaya, E.P., Kessler, V.G., Yanovskaya, M.I., "The Chemistry of Metal Alkoxides", Boston: Kluwer Academic Publishers, 107-125, (2002).

[45] Sharma, P.K., Varadan, V.V., Varadan, V.K., "A critical role of pH in the colloidal synthesis and phase transformation of nano size α-Al_2O_3 with high surface area", Journal of the European Ceramic Society, 23: 659–666, (2003).

[46] Sharma, P.K., Jilavi, M.H., Nass, R., Schmidt, H., "Tailoring the particle size from μm→nm scale by using a surface modifier and their size effect on the fluorescence properties of europium doped yttria", Journal of Luminescence, 82: 187–193, (1999).

[47] Gaweł, B., Gaweł, K., Øye, G., "Sol-gel synthesis of non-silica monolithic materials", Materials 3: 2815–2833, (2010).

[48] Khalil, K.M.S., "Formation of mesoporous alumina via hydrolysis of modified aluminum isopropoxide in presence of CTAB cationic surfactant", Applied Surface Science, 255: 2874–2878, (2008).

[49] Wang, Z.M., "Handbook of Nanophysics: Functional Nanomaterials", Sattler, K. D., USA: Taylor & Francis Group, 9.1-9.12, (2011).

[50] Scholten, J.J.F., "Studies in Surface Science and Catalysis", 79, Moulijn, J. A., van Leeuwen, P. W. N. M., van Santen, R. A., Amsterdam: Elsevier, 419-438, (1993).

[51] Sakka, S., "Handbook of Advanced Ceramics Materials, Applications, Processing, and Properties", Somiya, S., Amsterdam: Academic Press, 883-910, (2013).

[52] Yang, H., Han, R., Li, F., "Synthesis of mesoporous γ-alumina and its catalytic performance in dichloropropanol cyclization", Quimica Nova, 42: 851–858, (2019).

[53] Dubey, S., Singh, A., Nim, B., Singh, I.B., "Optimization of molar concentration of $AlCl_3$ salt in the sol–gel synthesis of nanoparticles of gamma alumina and their application in the removal of fluoride of water", Journal of Sol-Gel Science and Technology, 82: 468–477, (2017).